

TRIGGERED STAR FORMATION

Bruce G. Elmegreen¹

Abstract. Triggered star formation in bright rims and shells is reviewed. Shells are commonly observed in the Milky Way and other galaxies, but most diffuse shells seen in HI or the infrared do not have obvious triggered star formation. Dense molecular shells and pillars around HII regions often do have such triggering, although sometimes it is difficult to see what is triggered and what stars formed in the gas before the pressure disturbances. Pillar regions without clear age gradients could have their stars scattered by the gravity of the heads. Criteria and timescales for triggering are reviewed. The insensitivity of the average star formation rate in a galaxy to anything but the molecular mass suggests that triggering is one of many processes that lead to gravitational collapse and star formation.

1 Introduction: Large-Scale Shells

High resolution images of nearby spiral galaxies show large dust and gas bubbles in the spiral arms (Fig. 1; see also Fig. 3 in Lecture 2). Their radii are often larger than the gas scale heights, so these are unlikely to be spheres; they are more like rings in the disk. There are also feathers, comets, and other fine-scale dust structures in optical images – all indicating recent dynamical processes. Sometimes there are small bubbles inside large bubbles, and there are generally more bubbles near the spiral arms than in the interarm regions. The interarm also contains dust streamers, and many of these look like old bubbles left over from more active times in the arms.

Gould's Belt contains the Local Bubble, studied recently by Lallement et al. (2003) using Na I absorption clouds near the Sun. This local bubble is also a source of diffuse x-ray emission from hot gas (Snowden et al., 1998). Presumably the energy came from hot stars in the Sco-Cen association (Breitschwerdt & de Avellez, 2006).

¹ IBM T. J. Watson Research Center, 1101 Kitchawan Road, Yorktown Heights, New York 10598 USA, bge@us.ibm.com

Large bubbles in the Milky Way are also evident from IR maps of the sky. Könyves et al. (2007) used IRAS $60\mu\text{m}$ and $100\mu\text{m}$ images to identify Milky Way bubbles. They reported that the bubble volume filling factor in the inner galaxy is around 30%, and in the outer galaxy it is around 5%. Ehlerová & Palouš (2005) catalogued HI shells in the Milky Way using the Leiden-Dwingeloo Survey. They found a volume filling factor of 5%, a mean age of 8.4 Myr, and a ratio of age to filling factor equal to 170 Myr. This latter timescale is the time for the whole interstellar volume (not mass) to be cycled through one or another HI shell. This is 10 times faster than the time for molecular gas to be converted into stars. Since the shells observed by Ehlerová & Palouš are atomic, this ISM processing would seem to be independent of the molecular cloud population. The GMCs have a low volume filling factor and the HI shells occupy the space between them. A significant fraction of the HI shell mass can come from GMC disruption in the inner galaxy where the molecular fraction is high.

The LMC is also filled with large shells (Goudis & Meaburn, 1978). The largest, LMC4, has no obvious cluster or OB association in the center, although



Fig. 1. Region of the galaxy M51 viewed with the ACS camera of HST, showing bubbles.

there are A-type stars suggesting a ~ 30 Myr old age (Efremov & Elmegreen, 1998). It has pillars at the edge with young star formation, and an arc of young stars without gas in the center, called Constellation III (McKibben Nail & Shapley, 1953). Yamaguchi et al. (2001) studied the star formation in this region, pointing out GMCs and young clusters all along the edge of the shell and suggesting these were triggered.

IC 10 is another small galaxy filled with HI holes and shells. Wilcots & Miller (1998) found H α at the edges of the shells and discussed these young regions as triggered star formation. Similarly, the small galaxy IC 2574 has a giant shell with an old central cluster and triggered young stars on edge (Walter & Brinks, 1999; Connon et al., 2005).

2 Shell Expansion

Expanding shells are most commonly made by stellar pressures in the form of HII regions, supernovae, and winds. If we write the expansion speed as $dR/dt \sim (P/\rho)^{1/2}$ for an isothermal shock, then the radius varies as a power law in time if the pressure P is a function of radius R and the density ρ is uniform. For an HII region, $P = 2.1nkT$ where $n = (3S/4\pi R^3\alpha)^{1/2}$ for ionizing luminosity S in photons per second and recombination rate α to all but the ground state. Then $P \propto R^{-3/2}$. For supernovae, $P \sim 3E/4\pi R^3$ for the energy conserving, non-radiative, phase. For a wind, $P \sim 3E(t)/4\pi R^3$, where the energy increases with time as $E = Lt$.

These three pressure-radius relations give three different radius-time expansion laws, $dR/dt \propto R^{-3/4}$ gives $R \propto t^{4/7}$ for a Strömngren sphere, $dR/dt \propto R^{-3/2}$ gives $R \sim t^{2/5}$ for the Sedov phase of a supernova, and $dR/dt \propto t^{1/2}R^{-3/2}$ gives $R \propto t^{3/5}$ for a steady wind or continuous energy supply from multiple supernovae in an OB association (Castor et al., 1975).

There are many complications to these solutions. External pressure is always present, slowing down the bubbles. External pressure P_{ext} enters the expression as $dR/dt = ([P - P_{\text{ext}}]/\rho)^{1/2}$ with $P_{\text{ext}} \sim \text{constant}$. The solution is not a power law in this case. A second complication is the momentum in the moving shell. When this is important, the equation of expansion is really $d(4\pi R^3 v \rho/3)/dt = 4\pi R^2(P - P_{\text{ext}})$. Shell momentum makes the shell move faster at a given radius than in the case without momentum. There are also diverse shock jump conditions depending on the importance of magnetic fields and the equation of state for the shocked gas, such as adiabatic or isothermal, or whether the full energy equation is used to determine the post-shock temperature.

We can see how important external pressure is to these solutions by finding the fraction of shells that are at a pressure significantly above the external value. As noted above, each source has solutions $R(t)$ and $P(R)$, which can be re-written into a solution for pressure versus time, $P(t)$. Thus there is a relation for the volume as a function of pressure, $V(P)$. For a constant rate n_0 of making bubbles, $n(P)dP = n_0 dt$. Therefore $n(P) \propto dt/dP$. The volume filling factor is $f(P) = n(P)V(P)$. Now we see that for HII regions, $f(P) \propto P^{-4.17}$; for winds, $f(P) \propto P^{-4.5}$, and for supernovae, $f(P) \propto P^{-5.2}$. For all of these, approximately, $f(P)dP \propto AP^{-4.5}dP$

for some constant A . If all of the volume is filled, then $1 = \int f(P)dP$, and the average pressure is related to the minimum pressure as $P_{\text{ave}} = 1.4P_{\text{min}}$, which means $f(P) = 1.15(P/P_{\text{ave}})^{-4.5}/P_{\text{ave}}$. Thus, the probability that any of these regions has a pressure exceeding 10 times the average, $f(P > 10P_{\text{ave}})$, is $0.31 \times 0.1^{3.5} \sim 10^{-4}$; similarly, $f(P > 2P_{\text{ave}}) \sim 0.03$. Evidently, most pressure bursts from HII regions, winds and supernovae are within twice the average ISM pressure for most of their lives. Therefore the external pressure is important for them. Kim, Balsara & Mac Low (2001) ran numerical simulations of the ISM and found that most of the time, the pressure stayed within a factor of 2 of the average value.

The probability distribution function for pressure also suggests that the largest pressure bursts are close-range and short-lived. Thus significant over-pressures from stellar sources are most likely to occur close to those stars, as in an adjacent cloud. Most of the giant IR and HI shells discussed above are drifting by momentum conservation.

3 Triggering: Bright Rimmed Clouds and Pillars

HII regions interact with their neighboring molecular clouds by pushing away the lower density material faster than the higher density cloud cores. This leads to bright rims and pillars. Most HII regions contain these shapes, as they are commonly observed in Hubble Space Telescope images of nebulae. Triggered star formation in the dense heads of pillars has been predicted (e.g., Klein, Sandford & Whitaker, 1980) and observed for many years (e.g., Sugitani et al., 1989). Here we review some recent observations.

Recent simulations of bright rim and pillar formation are in Mellema et al. (2006), Miao et al. (2006), and Gritschneder et al. (2009). In a large HII region,

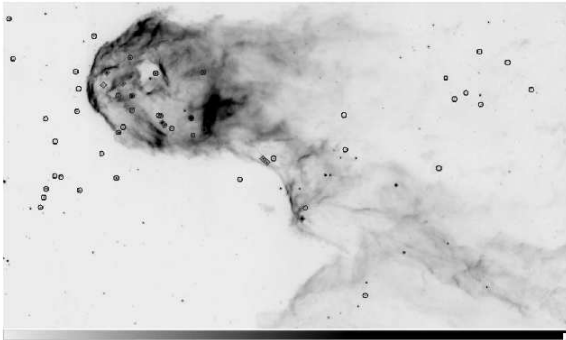


Fig. 2. A pillar in IC 1396 viewed at $8\mu\text{m}$ with the Spitzer Space Telescope. Class I sources (the youngest) are identified by diamond shapes. There are three at the front of the head, one near the back part of the head, two on the lower part of the pillar and another in a shelf nearby (from Reach et al. (2009)).

there can be many bright rims with star formation in them. A good example is 30 Dor in the LMC, which has bright-rims that look like they have triggered star formation in many places (Walborn, Maíz-Apellániz & Barbá, 2002).

IC 1396 is an HII region with a shell-like shape. The radius is 12 pc, and the expansion speed is 5 km s^{-1} , making the expansion time 2.5 Myr (Patel et al., 1995). The shell contains several bright rims and pillars around the edge that all point to the sources of radiation. In optical light, few embedded stars can be seen, but in the infrared there are often embedded stars.

The stellar content of the large pillar in IC 1396 has been studied by Reach et al. (2009; see Figure 2). Several Class I protostars are located in the main head and in a shelf off the main pillar. Class II stars are scattered all over the region with no particular association to the cloud. The Class I stars recently formed in the pillar, and considering that they are much younger than the HII region, they could have been triggered.

Getman et al. (2007) observed IC 1396N, another bright rim in the same region, in x-ray and found an age sequence that suggests triggering from south to north, into the rim. There are class III and class II stars around the rim and class I/0 stars inside. Beltrán et al. (2009) did a JHK survey of the same bright rim and found few NIR-excess sources and no signs of clustering toward the southern part of the rim. They also found no color or age gradient in the north-south direction. They concluded there was no triggering but perhaps there was a gradient in the erosion of gas around protostars. Choudhury et al. (2010) observed the region with Spitzer IRAC and MIPs and suggested there was an age sequence with the younger stars in the center of the bright rim and the older stars near the edge. They derived a propagation speed into the rim of $0.1 - 0.3 \text{ km s}^{-1}$.

The pillars of the Eagle Nebula, M16, are among the most famous cloud structures suggestive of triggering. Several young stars appear at the tips. It is difficult to tell if these stars were triggered by the pressures that made the pillars, or if they existed in the head regions before the HII pressure swept back the periphery. Triggering requires that the pillar stars are much younger than the other stars in the region. Some exposure of existing stars could be possible if there is a wide range of ages among the pillar and surrounding stars.

Sugitani et al. (2002) found Type I sources near the pillar heads in M16 and older sources all around the pillars. They suggested there was an age sequence within the pillar. Fukuda et al. (2002) observed M16 in ^{13}CO , C^{18}O , and 2.7 mm emission, finding a high density molecular core at the end of the pillar, as expected from HII region compression. However, Indebetouw et al. (2007) suggested that the young objects in the area are randomly distributed and not triggered. They showed the distribution of protostars in various stages of accretion and saw no clear patterns with age. Thus the issue of triggering in the M16 pillars seems unresolved.

Guarcello et al. (2010) found a different age sequence in M16: the stars in the northwest part of the whole HII region are younger than the stars in the southeast part. They suggested that a 200 pc shell triggered both M16 and M17 3 Myr ago on much larger scales.

4 Age Sequences in Bright Rims

Several of the references above look for or find age sequences of stars along the axis of a bright rim. Sugitani, Tamura & Ogura (1995) pioneered this. At first, such a sequence seems obvious because the HII region is expanding, so position correlates with time. However, the bright-rim heads are usually more massive than the stars and the stars should be gravitationally attracted to the heads. If the head acceleration by gas pressure is less than their internal acceleration by gravity, then the embedded stars will get pulled along with the heads as the heads move. There would be little exposure of the stars in that case. To accelerate the head faster than the internal gravitational acceleration means that the pressure difference between the front and the back side has to exceed the internal gravitational acceleration multiplied by the head column density. Both of these quantities are essentially the internal self-gravitational binding energy of the head if the head is virialized, and therefore also the internal turbulent energy density. In that case, the head has to be accelerated faster than the square of its turbulent velocity dispersion divided by its radius. Such a larger acceleration could occur when the initially low-density gas is first compressed into a comet head by the HII region. Once the entire head is compressed and star formation occurs in the dense gas, the inside of the head will be close to pressure equilibrium with the outside ionization front, and the relative acceleration will decrease.

A description of such pressure equilibrium and the resulting acceleration is given by Bertoldi & McKee (1990). In their equation 5.10, they write the ratio of the self-gravitational acceleration inside the head to the acceleration of the whole head by the rocket effect as

$$\frac{g_{\text{grav}}}{g_{\text{rocket}}} \sim 2 \left(\frac{M_{\text{cl}}}{M_{\text{Jeans}}} \right)^{2/3} \quad (4.1)$$

for a non-magnetic head, and

$$\frac{g_{\text{grav}}}{g_{\text{rocket}}} \sim \left(\frac{M_{\text{cl}}}{M_{\Phi}} \right)^2 \quad (4.2)$$

for a magnetic head. Here, M_{cl} is the cloud head mass, $M_{\text{Jeans}} = 1.18\sigma_{\text{cl}}^4/(G^3 P_{\text{cl}})^{1/2}$ and $M_{\Phi} = 0.12\Phi/G^{3/2}$ are the critical (or maximum) cloud masses for stability without and with a magnetic field, respectively; Φ is the total magnetic flux in the cloud. The pressure at the ionized surface of the cloud enters the expression for M_{Jeans} and is

$$\frac{P_{\text{cl}}}{k} = 2.45 \times 10^7 [S_{49}/(R_{\text{cl,pc}} R_{\text{pc}}^2)]^{1/2} \text{ cm}^{-3} K \text{ if } (\psi > 10) \quad (4.3)$$

$$= 1.65 \times 10^9 (S_{49}/R_{\text{pc}}^2) \text{ cm}^{-3} K \text{ if } (0.3 < \psi < 10) \quad (4.4)$$

for dimensionless parameter ψ ,

$$\psi = \alpha F_{\text{II}} R_{\text{cl}} / \sigma_{\text{II}}^2 = 5.15 \times 10^4 \frac{S_{49} R_{\text{cl,pc}}}{R_{\text{pc}}^2}. \quad (4.5)$$

In these expressions, the recombination rate to all but the ground state is α , the incident ionizing flux is F_{II} in photons $\text{cm}^{-2} \text{s}^{-1}$, the ionizing luminosity is S_{49} in photons s^{-1} , the cloud radius is $R_{\text{cl,pc}}$ in pc, the distance to the ionizing source is R_{pc} , in pc, the velocity dispersion in the cloud is σ_{cl} , and the velocity dispersion in the HII region is σ_{II} .

These equations suggest that if the cloud head requires gross instability for a star to form, i.e., $M_{\text{cl}} > M_{\text{Jeans}}$ or $M_{\text{cl}} > M_{\Phi}$ (or, $M_{\text{cl}} > M_{\text{Jeans}} + M_{\Phi}$ in McKee (1989), then the internal gravitational acceleration in the head is always greater than the rocket acceleration. Thus the stars that form in the head should follow the head along as it accelerates away from the HII region. Why are the stars “left behind” in this case?

Another consideration is that the side of the dense core facing the HII region could be continuously peeled away by the ionization. The speed of this peeling is determined by the incident flux. After pressure equilibrium, a D-type ionization front enters the compressed neutral gas; “D” stands for density-bounded, i.e., the ionizing radiation is stopped by gas absorption (Spitzer, 1978). The speed of such a front into the dense gas is $\sigma_{\text{cl}}^2/[2\sigma_{\text{II}}]$. Because $\sigma_{\text{II}} \gg \sigma_{\text{cl}}$, this D-front speed is always much less than σ_{cl} . The orbit speed of a newly formed star inside the head is of order σ_{cl} , however, for a self-gravitating head. Thus the speed at which the ionized side of the pillar gets peeled away is always much less than the embedded stellar speed. Thus, stars should not be exposed by ionization either.

Evidently, for both the rocket effect and ablation by ionization, stars forming in an unstable head should continuously fall back into the head center faster than the surface of the head moves away from the source of ionization. This makes the exposure of young stars and their age gradients difficult to understand. It could explain, however, why age gradients are seldom obvious – the triggered stars scatter around the head by gravitational forces.

One solution to this problem is that the head is stable on a large scale with σ_{cl} equal to some turbulent speed that is larger than the sound speed, or perhaps with magnetic support, and yet inside of the head, there are local dense clumps that are unstable in the sense that their masses are larger than the thermal Jeans mass after the magnetic field has diffused out. In these cases, it might be possible that $M_{\text{core}} > M_{\text{Jeans,thermal}}$ for localized star formation while at the same time $g_{\text{grav}} < g_{\text{rocket}}$ for exposure of the star after it forms.

Another model of triggered star formation is that there is a pre-existing pillar-like shape with multiple clumps aligned to the HII region. Then the compression front moves along the pillar from clump to clump, triggering gravitational instabilities as it goes. The exposure of the stars would follow the erosion of each clump, compressed one after another.

Of course it is possible that the stars near the head were not triggered. A key observation for triggering will be the velocities of the young stars near the head in comparison to the head velocity. If the stars are moving much slower than the head, then they could have formed before the compression and rocket-like acceleration.

Simulations by Dale et al. (2007b) of triggered star formation in numerous

dense clumps of a pre-existing molecular cloud indicate the difficulty in distinguishing between stars that formed previously and were exposed by clump ionization or motion, and stars that were triggered by the ionization pressure. In this study, the additional amount of star formation that was from the triggering alone was only $\sim 30\%$.

5 Shell Expansion: Collect and Collapse

Zavagno et al. (2006) studied star formation in the Milky Way source W 79 (Fig. 4). It has a 1.7 Myr old shell with gravitationally collapsed regions 0.1 Myr old along the perimeter. This is an example of star formation triggering by the gravitational collapse of swept-up gas around an older cluster or OB association. Sh2-219 is a similar region (Deharveng et al., 2006). There is O9.5V star in a centralized HII region, and a CO cloud, K-band embedded cluster, Ultra-compact HII region, and Herbig Be star at the edge.

Deharveng et al. (2010) recently studied 102 bubbles and triggered star formation using the Spitzer-GLIMPSE and MIPS GAL surveys for the IR, the MAGPIS and VGPS surveys for the radio continuum, and the ATLASGAL survey at $870 \mu\text{m}$ for cold dust emission. They found that 86% of the bubbles contain HII regions, and among those with adequate resolution, 40% have cold dust along their bor-

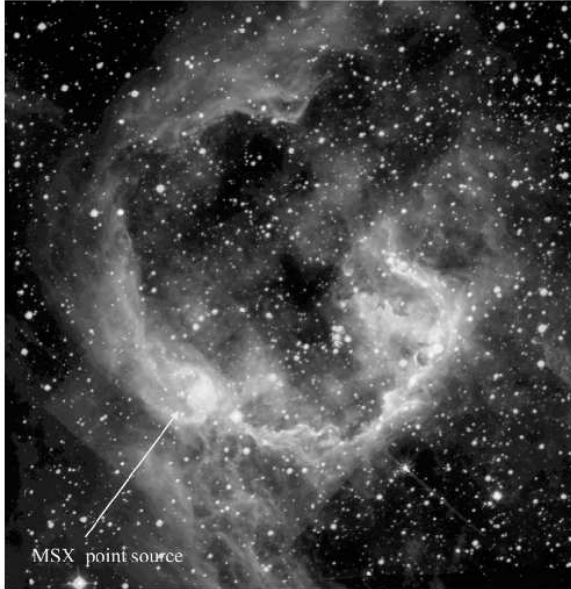


Fig. 4. Milky Way region W 79, consisting of a shell with dense clouds and star formation at the edge, from Zavagno et al. (2006).

ders, presumably accumulated during the bubbles' expansions. Eighteen bubbles have either ultracompact HII regions or methanol masers in the peripheral dust, indicating triggering. They categorized their results into several types of triggering. Star formation that occurs in pre-existing cloud condensations is distinctive because the clouds protrude into the bubble cavity like bright rims; 28% of the resolvable shells are like this. Star formation that occurs by the collapse of swept-up gas does not protrude but is fully in the shell. That is because it is comoving with the shell. In fact, clumps forming by gravitational collapse in a shell could eventually protrude out of the front of the shell because their higher column densities makes them decelerate slower than the rest of the shell (Elmegreen, 1989). If this is observed, then the relative position of a triggered clump and the shell around it should indicate their relative speeds and the time when the clump first formed.

Beerer (2010) studied Cygnus X North with Spitzer IRAC, classifying stars according to their IR spectral ages. They found that younger objects are in filaments that look compressed. Triggering of those stars was suggested.

Desai (2010) examined all 45 known supernova remnants in the LMC and looked for associations with young stellar objects and with GMCs that have no YSOs. Seven SNRs were associated with GMCs and YSOs, 3 SNRs were with YSOs and no GMCs, and 8 SNRs were with GMCs and no YSOs. For the 10 SNRs with YSOs, only 2 have YSOs that are clearly associated with the SN shell, but in these cases, the SNe are younger than YSOs, so the YSOs could not have been triggered. Desai et al. concluded that SNe are too short-lived for triggering.

6 General Aspects of Triggering

Gas expands away from long-lived pressure sources like HII regions and OB association bubbles. If the expansion scale is smaller than the scale of a single cloud or the distance to a nearby cloud, then pillars and bright rims form by the push-back of interclump gas. In this case, star formation is a relatively fast process that works by squeezing the pre-existing dense gas. The velocity of the triggered stars is smaller than the overall shell expansion speed. The time delay between the beginning of the pressure source and the formation of new stars is the time for the pressure disturbance to reach the pre-existing cloud, i.e., the HII region expansion time, plus the time for the pressure to implode the cloud, which is relatively fast.

If the expansion scale is larger than the scale of a single cloud, then shells form by the push-back of most nearby gas. A cavity then forms with accumulated dense gas at the edge. This process of triggering is relatively slow because new clumps have to form by gravitational instabilities in the swept-up gas. The timescale for collapse and the properties of shells when they collapse were investigated by Elmegreen et al. (2002) using collapse criteria in Elmegreen (1994). They ran several thousand models of expanding shells in rotating, shearing galaxies and found various trends with environmental factors. The basic time scale for triggering was

$$t \sim 4\xi^{1/10}(2\pi G\rho_0)^{-1/2}, \quad (6.1)$$

where $\xi = \sigma^5/GL$ for source luminosity L and sound speed σ in the shell, and for pre-shell density ρ_0 . They also found that the probability of collapse, or the fraction of shells that collapse, f , depends on the Toomre Q parameter for all possible variations in environment (see Lecture 1). The relation is $f \sim 0.5 - 0.4 \log_{10} Q$.

Simulations of shell formation and collapse around HII regions were made by Hosokawa & Inutsuka (2005, 2006a,b) and Dale et al. (2007a). Hosokawa & Inutsuka (2006a) found that shells driven into molecular clouds at typical densities have time to fragment and form new stars. They showed that at low ambient densities, the fragmentation can occur before CO forms, but at high densities, the shell is primarily CO. Hosokawa & Inutsuka (2006b) considered the minimum stellar mass that drives an expansion in which triggered star formation produces a second generation mass comparable to or larger than the first star; this stellar mass is around $20 M_{\odot}$ for a pre-shock density of 100 cm^{-3} . Dale et al. (2007a) ran several simulations of an expanding HII region into a molecular cloud and compared the resulting radii and times for collapse with the analytical theory by Whitworth et al. (1994), which represented the numerical results well.

For the collect and collapse process, the velocity of triggered stars in the swept-up region can be large, $\sim (P/\rho_0)^{1/2}$ for driving pressure P and ambient density ρ_0 . Evidence for triggering involves the causality condition: the triggering distance, age difference, and relative velocity of the triggered stars compared to the pressure-driving stars has to satisfy the relationship that the distance equals the velocity times the time. The triggered stars have to be much younger than the pressure-driving stars, and there has to be a clear age bifurcation into triggering star ages and triggered star ages, in order to be certain that triggering has occurred. Without a clear age difference, the suspected triggered stars could be part of the overall star formation process in the first generation, even if they are located in a compressed clump near the edge of the pressurized region.

Simulations of star formation triggered by ionization pressure have been discussed by Dale et al. (2005, 2007b) and Gritschneider et al. (2009). These simulations run for too short a time to generate an expanding coherent shell and form stars by the collect and collapse mechanism. Triggering instead is by the forced compression of pre-existing clumps. Because stars are forming in these clumps anyway, the excess star formation from triggering is small. Longer-time simulations could show more triggering in the collect and collapse scenario. As mentioned above, the timescale has to be several times the dynamical time in the pre-shock material. This is a problem for clouds that are not magnetically supported because they will collapse anyway in that time, even without compression. Thus triggering, as observed in shells, requires stability before the compression arrives, presumably from magnetic forces, and instability after the compression, presumably from enhanced magnetic diffusion in the compressed region combined with a greater surface pressure for the given cloud mass.

Thick shells should differ from thin shells in their stability properties because the gravitational forces in the shell are diluted by thickness when it is large, as discussed for galactic disks in Section 1.1 of Lecture 1. Wunsch (2010) studied the

thick shell case for shells that do not accumulate material as they expand, but are bound on both sides by thermal pressure.

7 ISM Energy Sources that may Trigger Star Formation

There are many energy sources for the ISM but only a few are likely to trigger star formation. The essential condition is that the energy source has to change a cloud from stable to unstable. Usually this requires some kind of compression, the compressed mass has to exceed an unstable mass, and the compressive force has to last for a time comparable to the collapse time in the compressed region. As mentioned above, individual supernova seem too short-lived to trigger star formation in the ambient ISM, even though they play an important role in energizing the ISM. More important are the HII regions, stellar winds bubbles, and multiple supernovae that occur in OB associations and star complexes. Another long-range and long-lived source of compression is a spiral density wave.

8 Summary

As we have seen over the last four lectures, star formation can be initiated by a variety of processes, including spontaneous gravitational instabilities in the combined stellar and gaseous medium, occasional cloud collisions, especially in density-wave shocks, and triggered gravitational instabilities in compressed regions ranging from spiral-arm dust lanes, to Lindblad resonance rings, tidal arcs around interacting galaxies, gaseous shells and rings in galactic disks, and molecular clouds at the edges of HII regions. The role of compression is either to bring some amount of otherwise stable gas together so it can collapse and form stars on its own, or to compress an existing cloud from a stable configuration to an unstable configuration, at which point it, too, forms stars on its own. Always accompanying this gas redistribution or compression is an enhancement in internal energy dissipation. Otherwise, the region would have collapsed into stars on its own. Compression through a shock does this reduction, or compression-enhancement of magnetic diffusion, or even compression to reduce the turbulent dissipation time. Without compression, the region may still collapse on its own, but with a longer time scale.

Because the final step in all of these triggering scenarios is the formation of stars deep in a cloud core, away from any pressure source that may be acting on the cloud surface, the detailed processes of star formation, such as stellar collapse, accretion, disk formation, and so on, should not depend much on triggering. If the source of compression also heats the gas, then perhaps the thermal Jeans mass increases in the compressed region, and this might affect the stellar initial mass function. However, higher driving luminosities and therefore higher cloud temperatures are usually accompanied by higher pressures in a way that the thermal Jeans mass stays about constant (Elmegreen et al., 2008).

The overall affect of triggered star formation on the average star formation rate seems to be small in the main parts of galaxy disks. The empirical laws discussed

in Lecture 1 seem not to depend on how the self-gravitating molecular gas is made, as long as it is made quickly between previous molecular cloud disruptions. If the dispersed gas from a previous event of star formation lingers around in a diffuse state for a long time, without forming stars, then it might still turn molecular from self-shielding, thereby contributing to Σ_{H_2} , but not contribute in the right proportion to Σ_{SFR} . The empirical Bigiel et al. (2008) law would then fail. We suggested in Lecture 2 that this may be the case for dust clouds in the interarm regions of M51, i.e., that they are marginally stable to have lasted so long from their formation in the previous spiral arm. But the fraction of molecules in a non-gravitating form cannot be large for the correlation between Σ_{SFR} and Σ_{H_2} to work out as well as it does. Frequent gas compression by all of the various pressures in the ISM, combined with the forced loss of internal energy that accompanies this compression, ensures that most of the molecular and atomic debris from one event of star formation soon makes it into another event of star formation. Prevalent triggering thereby acts as a scavenger for inert diffuse clouds, keeping most parts of the ISM in a constant state of collapse or imminent collapse. This is the saturation in star formation that previous lectures have mentioned.

With very low star formation rates, as in dwarf galaxies and the outer parts of disks, a much higher fraction of the gas can be in diffuse form, and then triggering can play a more direct role in the average star formation rate. At a very minimum, it can provide locally high pressures where the thermal stability of the gas allows a cool phase to exist in equilibrium with the radiation field. Without such cool phases, disk instabilities will just make warm and diffuse flocculent spirals in the gas, and there will not be enough dense matter to affect the star formation rate. Put simply, at very low average pressures, cool diffuse clouds seem to require pressure disturbances for their formation from the warm phase. Most commonly, outer spiral arms seem to do this, but stellar pressure sources might be important too. This enablement of cool cloud formation is presumably the first step in the condensation process that leads to star formation.

References

- Beerer, I.M. 2010, ApJ, 720, 679
- Beltrán, M. T., Massi, F., López, R., Girart, J. M., & Estalella, R. 2009, A&A, 504, 97
- Bertoldi, F., & McKee, C.F. 1990, ApJ, 354, 529
- Bigiel, F., Leroy, A., Walter, F., Brinks, E., de Blok, W. J. G., Madore, B., & Thornley, M. D. 2008, AJ, 136, 2846
- Breitschwerdt, D., & de Avillez, M. A. 2006, A&A, 452, L1
- Castor, J., McCray, R., & Weaver, R. 1975, ApJ, 200, L107
- Choudhury, R., Mookerjea, B., & Bhatt, H. C. 2010, ApJ, 717, 1097

- Connon et al. 2005, ApJ, 630, L37
- Dale, J. E., Bonnell, I. A., Clarke, C. J., & Bate, M. R. 2005, MNRAS, 358, 291
- Dale, J. E., Bonnell, I. A., & Whitworth, A. P. 2007a, MNRAS, 375, 1291
- Dale, J. E., Clark, P. C., & Bonnell, I. A. 2007b, MNRAS, 377, 535
- de Geus, E. 1992, A&A, 262, 258
- Deharveng, L., Schuller, F., Anderson, L. D., Zavagno, A., Wyrowski, F., Menten, K. M., Bronfman, L., Testi, L., Walmsley, C. M., & Wienen, M. 2010, arXiv1008.0926
- Deharveng, L., Lefloch, B., Massi, F., Brand, J., Kurtz, S., Zavagno, A., & Caplan, J. 2006, A&A, 458, 191
- Desai, K.M. 2010, AJ, 140, 584
- Efremov, Yu.N., & Elmegreen, B.G. 1998, MNRAS, 299, 643
- Ehlerová, S., & Palouš, J. 2005, A&A, 437, 101
- Elmegreen, B.G. 1989, ApJ, 340, 786
- Elmegreen, B.G. 1994, ApJ, 427, 384
- Elmegreen, B. G., Palouš, J., & Ehlerová, S. 2002, MNRAS, 334, 693
- Elmegreen, B.G., Klessen, R., & Wilson, C. 2008, ApJ, 681, 365
- Fukuda, N., Hanawa, T., Sugitani, K. 2002, ApJ, 568, L127
- Getman, K.V., Feigelson, E.D., Garmire, G., Broos, P., & Wang, J. 2007, ApJ, 654, 316
- Goudis, C., Meaburn, J. 1978, A&A, 68, 189
- Gritschneider, M., Naab, T., Walch, S., Burkert, A., & Heitsch, F. 2009, ApJ, 694, L26
- Guarcello, M. G., Micela, G., Peres, G., Prisinzano, L., & Sciortino, S. 2010, A&A, 521, 61
- Hosokawa, T., & Inutsuka, S-I. 2005, ApJ, 623, 917
- Hosokawa, T., & Inutsuka, S-I. 2006a, ApJ, 646, 240
- Hosokawa, T., & Inutsuka, S-I. 2006b, ApJL, 648, 131
- Hosokawa, T. & Inutsuka, S.-I. 2007, ApJ, 664, 363

- Indebetouw, R., Robitaille, T. P., Whitney, B. A., Churchwell, E., Babler, B., Meade, M., Watson, C., & Wolfire, M. 2007, *ApJ*, 666, 321
- Kim, J., Balsara, D., & Mac Low, M.-M. 2001, *JKAS*, 34, 333
- Kirk, J. M., Ward-Thompson, D., & André, P. 2005, *MNRAS*, 360, 1506
- Klein, R.I., Sandford, M.T., & Whitaker, R.W. 1980, *Space Sci. Rev.* 27, 275
- Könyves, V., Kiss, Cs., Moór, A., Kiss, Z. T., & Tóth, L. V. 2007, *A&A*, 463, 1227
- Lada, C.J., Alves, J., & Lada, E.A. 1999, *ApJ*, 512, 250
- Lallement, R., Welsh, B. Y., Vergely, J. L., Crifo, F., & Sfeir, D. 2003, *A&A*, 411, 447
- Lombardi, M., Lada, C. J., & Alves, J. 2008, *A&A*, 489, 143
- McKee, C.F. 1989, *ApJ*, 345, 782
- McKibben Nail V., & Shapley H., 1953, *Harvard Rep.* 373
- Mellema, G., Arthur, S.J., Henney, W.J., Iliev, I.T., & Shapiro, P.R. 2006, *ApJ*, 647, 397
- Miao, J., White, G.J., Nelson, R., Thompson, M., & Morgan, L. 2006, *MNRAS*, 369, 143
- Patel, N.A., Goldsmith, P.F., Snell, R.L., Hezel, T., & Xie, T. 1995, *ApJ*, 447, 721
- Reach, W.T., et al. 2009, *ApJ*, 690, 683
- Smith, N. 2010, *MNRAS*, 406, 952
- Snowden, S., Egger, R., Finkbeiner, D. P., Freyberg, M. J., & Plueinsky, P. P. 1998, *ApJ*, 493, 715
- Spitzer, L. Jr., 1978, in *Physical Processes in the Interstellar Medium*, New York: Wiley,
- Sugitani, K., Fukui, Y., Mizuni, A., & Ohashi, N. 1989, *ApJL*, 342, 87
- Sugitani, K., Tamura, M., & Ogura, K. 1995, *ApJL*, 455, 39
- Sugitani, K., et al. 2002, *ApJ*, 565, L25
- Yamaguchi, R., Mizuno, N., Onishi, T., Mizuno, A., Fukui, Y. 2001, *ApJ*, 553, L185
- Walborn, N.R., Maíz-Apellániz, J., & Barbá, R.H. 2002, *AJ*, 124, 1601
- Walter, F., & Brinks, E. 1999, *AJ*, 118, 273

Whitworth A. P., Bhattal A. S., Chapman S. J., Disney M. J., & Turner J. A.,
1994, MNRAS, 268, 291

Wilcots, E.M., & Miller, B.W. 1998, AJ, 116, 2363

Wünsch, R., Dale, J. E., Palouš, J., & Whitworth, A. P. 2010, MNRAS, 407, 1963

Zavagno, A., Deharveng, L., Comerón, F., Brand, J., Massi, F., Caplan, J., &
Russeil, D. 2006, A&A, 446, 171